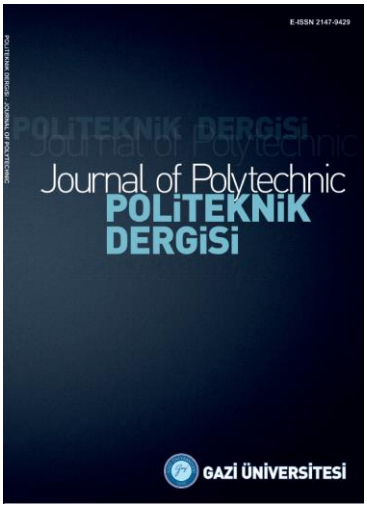

POLİTEKNİK DERGİSİ

JOURNAL of POLYTECHNIC

ISSN: 1302-0900 (PRINT), ISSN: 2147-9429 (ONLINE)
URL: http://dergipark.org.tr/politeknik

Accelerometer mass loading study based on a damage identification method using fundamental laws in closed systems

Kapalı sistemlerde temel kanunlar kullanılarak hasar tespit metoduna dayalı ivmeölçer kütle çalışması

***Yazar(lar) (Author(s))**: Tarık TUFAN[1], Hasan KÖTEN[2]*

ORCID[1]: 0000-0001-9324-2401

ORCID[2]: 0000-0002-1907-9420

To cite to this article: Tufan T. ve Köten H., "Accelerometer mass loading study based on a damage identification method using fundamental laws in closed systems", ***Journal of Polytechnic***, 26(2): 569-582, (2023).

Bu makaleye şu şekilde atıfta bulunabilirsiniz: Tufan T. ve Köten H., "Accelerometer mass loading study based on a damage identification method using fundamental laws in closed systems", ***Politeknik Dergisi***, 26(2): 569-582, (2023).

Erişim linki (To link to this article): http://dergipark.org.tr/politeknik/archive

DOI: **10.2339/politeknik.810768**

Accelerometer Mass Loading Study Based on a Damage Identification Method using Fundamental Laws in Closed Systems

Highlights

- *A New Indicator for damage detection*
- *The effect of accelerometer mass on the damage indicator was examined*
- *It has been discussed that large systems with mass change such as bridges can be considered as closed systems*

Graphical Abstract

In this study, it is aimed to show that damage can be identified successfully in closed systems with an accelerometer whose weight cannot be neglected. In addition, the effect of accelerometer mass on the damage parameter was also investigated.

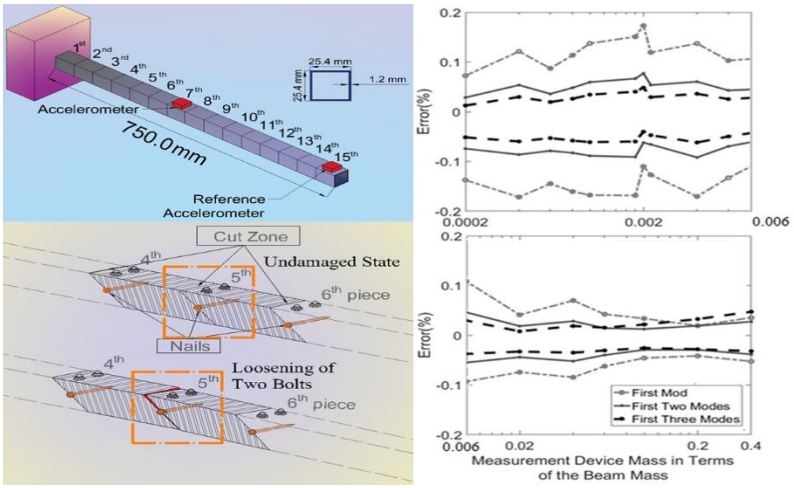

Figure. Summary showing Accelerometer orientation in the system, Damage in Experiment, and Accelerometer weight effect

Aim

Damage detection in the closed system.

Design & Methodology

An analytical system and a real system in which the damage is easily identified were used, and system was identified with Modal Plot, and the location of the damage was determined with the proposed damage parameter.

Originality

A new damage indicator which is successful also in closed systems.

Findings

In the analytical study, a 100-element 200 degree of freedom fixed-free beam is investigated and the assessment of the damage position is verified numerically and the validity of the parameter is examined in an experimental study.

Conclusion

It is observed that the accelerometer mass does not have a serious effect if the damage is between the middle element and the fixed part.

Declaration of Ethical Standards

The author(s) of this article declare that the materials and methods used in this study do not require ethical committee permission and/or legal-special permission.

Kapalı Sistemlerde Temel Kanunlar Kullanılarak Hasar Tespit Metoduna Dayalı İvmeölçer Kütle Çalışması

(Bu çalışma ECRES 2020 konferansında sunulmuştur. / This study was presented at ECRES 2020 conference.)

Araştırma Makalesi / Research Article

Tarık TUFAN*, Hasan KÖTEN

Mühendislik ve Doğa Bilimleri Fakültesi, İnşaat Mühendisliği Bölümü, İstanbul Medeniyet Üniversitesi, İstanbul

(Geliş/Received : 15.10.2020 ; Kabul/Accepted : 19.11.2021 ; Erken Görünüm/Early View : 20.12.2021)

ÖZ

Temel süreklilik ve enerji denklemlerine göre pek çok inşaat mühendisliği yapısı kütle konum değişimine elverişli olan kapalı sistem olarak değerlendirilebilir. Yoğun trafik saatleri göz önüne alındığında, araç kütlesinin köprü üzerindeki konumunun değişken olduğu, ancak toplam kütlenin sabit kaldığı varsayılabilir. Bu çalışmada, sabit kütle dağılımına sahip sistemler için geçerli olan bir hasar göstergesi kullanılarak kapalı sistemlerdeki hasarın başarıyla tahmin edilebileceğinin gösterilmesi amaçlanmıştır. Analitik çalışmada, 100 elemanlı 200 derecelik serbest sabit serbest kiriş incelenmiş ve hasar pozisyonunun tespit edilebileceği sayısal olarak doğrulanmış ve parametrenin geçerliliği deneysel bir çalışmada incelenmiştir. Kirişin serbest ucundaki parça hariç; Hasarlı elemanlar üzerinden hesaplanan hasar göstergesinin, hasarsız elemanlarda hesaplanan hasar göstergesinin 60 katı olduğu tespit edilmiştir. Kirişin serbest ucundaki elemanlarda; ivmeölçerin kütlesine bağlı olarak bu oranın 6 ile 40 arasında olduğu görülmüştür. Bu nedenle, ivmeölçer kütlesi ve hasar göstergesi için bir kıstas önerilmiştir.

Anahtar Kelimeler: Sistem tanımlama, modal plan, hasar tespit, ivme ölçer kütlesi, yapı malzemesi.

Accelerometer Mass Loading Study Based on a Damage Identification Method using Fundamental Laws in Closed Systems

ABSTRACT

Many civil engineering structures can be evaluated as closed systems in which additional mass spatial distribution can change within the system in terms of the fundamental continuity and energy equations. Considering the heavy hours of traffic, it can be assumed that the position of the vehicle mass on the bridge is variable, but the total mass remains constant. This study aims to show that the damage to the closed systems can be successfully estimated by using a damage indicator that is valid for systems with constant mass distribution. In the analytical study, a 100-element 200 degree of freedom fixed-free beam is investigated and the assessment of the damage position is verified numerically and the validity of the parameter is examined in an experimental study. Except for the piece at the free end of the beam; It has been determined that the damage indicator calculated on the damaged elements is 60 times larger than the damage indicator calculated at the undamaged elements. In the elements at the free end of the beam; it was observed that this ratio is between 6 and 40 depending on the mass of the accelerometer. Therefore, a criterion for accelerometer mass and damage indicator is proposed.

Keywords: System identification, modal plot, damage detection, accelerometer mass loading, structural material.

1. INTRODUCTION

During the operation of the civil structures, the total mass of the structure may change. However, it can be assumed that the mass in the system is preserved within a certain period but the position of mass inside the system may change due to live loads inside the system. Hence, such a system can be considered as a closed system where energy transfer is possible and the mass in the system is displaced, provided that the total mass is preserved.

Real structures should be considered as closed systems that allow mass position change rather than mass position fixed systems. For example, bridges are systems that allow mass entry and exit (Figure 1). Therefore, it may be considered not suitable for a closed system. However, if the vehicles entering and leaving the bridge are negligible compared to the vehicle mass on the bridge, the bridges can be considered as closed systems with this assumption. It would be beneficial to model multi-story car park buildings and high-rise buildings as a closed system.

To ensure the sustainability of the utilization of large-scale buildings, bridges, high-rise buildings, government buildings, hospitals, libraries, and historical artifacts, it is important to inspect the occurrence of damage. Such critical structures become unusable at an unexpected time

*Sorumlu Yazar (Corresponding Author)
e-posta : tarik.tufan@medeniyet.edu.tr

[1]. Therefore, It is crucial to monitor the existence, location, and type of the extending defects to take proper precautions before the growths in defects reach one or more of the following critical levels: (i) disturbing the operational state of a structure, (ii) disrupting the "health" of a structure, (iii) endangering the surrounding living and nonliving environment [2]. Moreover, anticipating the wear on these structures and its timely intervention is an important step to prevent serious structural damage. It is possible to determine the condition of the system with different methods with structural health monitoring systems (SHM) [3]. One of these methods is the system or modal identification by taking acceleration records over the structure. It is important to use a proper method to accurately determine the modal parameters. One of the methods is the Modal Plot [4] approach which utilizes any of the Frequency Response Function (FRF) or Output-only observer/Kalman filter identification (O3KID) [5] methods. With the Modal Plot approach, the existence of the damage could be expressed with a pattern in the modal parameter estimates [4].

Figrure 1. (İBB TV) Light vehicle traffic over the 15 Temmmuz Şehitler Bridge

Damage can be defined as a thermo-mechanical phenomenon. Generally, micro defects may turn into macro defects over time or under various types of loading. Damage indicators are used to determine the defects and damages that will occur in the system. Many different damage parameters were proposed in the early days, and it is seen that a significant part of these damage parameters is the functions of the modal parameters [6]. Later, it is seen that such damage markers used in advanced methods such as artificial neural networks [7,8] and deep learning [9] are tried to be associated with damage in real structures. For a damage indicator to be used in real structures, it is essential to show that it can be used effectively in theoretical systems.

The estimation of damage indicators from the data is important. If the damage parameters, which are functions of the modal variables, are considered, it is not possible to calculate the actual values of the modal parameters in real structures since the external forces acting on the system may move away from the assumption of ambient vibration [10-12], or measurement errors may occur in measurement devices, and the measurement duration may be improper. However, it is possible to estimate very approximate modal parameters. In theoretical studies, modal parameters can be calculated by using system properties, thus eliminating system identification errors. Moreover, considering the error-free damage indicator, there may be factors that make it difficult to determine the defect or damage [13]. For example, the mass of the measuring device used is one of the factors that cause the error. Accelerometers, as mentioned, are a measuring device frequently used in structural health monitoring. Although the effects of accelerometer mass loading on mode variables have been discussed many times before [14, 15], it is seen that the uncertainty at the point of damage detection has not been discussed before in the literature.

To sum up, in literature, there is a need for a proper damage indicator. In this study, it is aimed to show that a method developed for systems where mass distribution does not change is valid also in closed systems. It was observed that there is a difference in the damage indicator according to the accelerometer mass at the boundary conditions of the system examined. A criterion is developed for the utilization of the damage indicator according to the accelerometer mass. To the extent of our knowledge, the selection of the accelerometer mass according to a damage detection procedure is novel for the literature. The validity of the damage identification method for the closed systems is numerically proved and supported with an experimental study. Moreover, modal plots, which is a tool to monitor modal excitation energy, are also constructed by utilizing FRF in this study.

2. DAMAGE DETECTION

Inelastic deformation processes of solid bodies represent thermo-mechanical processes due to the involved dissipation of mechanical work which is also true in such cases when the process runs isothermally [16]. The Inelastic deformations in steel, many ceramics and, aggregate stem from dislocations along slip planes are usually accompanied by certain damage processes due to micro-defects. These damage processes may start at a certain stage of the deformation process and result in the development of macro-defects in the materials [17]. In many cases, larger inelastic deformations are accompanied by certain irreversible damage processes which also have to be considered as thermo-mechanical processes [16].

$$\dot{w}_t = \dot{w}_e + \dot{w}_\iota \tag{1}$$

where $\dot{w}_t$ denotes inelastic work rate, $\dot{w}_e$ shows the dissipated part of the $\dot{w}_t$, and $\dot{w}_\iota$ represent the non-dissipated part of $\dot{w}_t$ which corresponds to thermodynamical processes.

For the structural health monitoring concerns, the input forces acting on the system provide the energy to excite the global and local modes of the system, but these loads also drive different types of damage mechanisms, which is thermo-mechanical processes as mentioned, in the

material according to a certain threshold value. As far as structural health monitoring targets are concerned, damage assessment can be classified under four main headings [18, 19]: Determining the Existence (Level 0), Location (Level 1) and, Severity (Level 2) of the Damage, and predicting the useful life of the system (Level 3).

Depending on the application, the type of damage [20] can be considered with level 0, or it can be considered as a new heading between damage location and damage severity levels.

Many studies are directly targeting level 1, skipping level 0. However, it is more meaningful to try to solve the level 1 problems after investigating the damage existence problem. In the experimental part of this study, the location of the damage of the beam with hinges, whose damage is detected in a previous study [4], is made with a numerically verified damage indicator.

2.1 Sensitivity Based Damage Identification Methods

Studies that relate changes in modal variables to the damage are called sensitivity-based methods. In the first years of the SHM studies, it was believed that one formula or definition will be appropriate for all kinds of structures like offshore platforms, towers, and buildings; the definition of damage levels expressed by Rytter [18] also is a reflection of this idea. This is one of the reasons why significant efforts were spent on sensitivity methods. Supposing that using one method for all types of structures may still be a possibility, data from experiments discourage hopes in the sensitivity-based methods and the "one method for all systems" concept. In this thesis, one way for the utilization of a sensitivity-based method is shown in damage detection for different types of structures. Some of the important studies in the literature are stated as follows:

The initial studies of damage detection are initiated by the association of the natural-frequency changes with changes in the mass or stiffness matrix. Researchers start with natural frequencies, which are easily estimated with high confidence, as modal parameters in damage detection problems. Because the natural frequencies do not contain geometric information, their use often comes to the fore in the Level 0 applications where the presence of the damage is to be detected. However, several studies attempt to identify the location of the damage using the first six or more natural frequencies: In the articles [23, 24], a method is proposed to estimate the damage location and extent using only natural frequencies on numerical structure model. Using the conservation of energy principle and assuming damage stems from a change in stiffness while ignoring changes in the system mass, a relation between member stiffness change and natural frequency change for a single member is derived by:

$$\Delta\omega_j^2 = \frac{\varepsilon_i^T(\Phi_j)\Delta k_i \varepsilon_i(\Phi_j)}{\Phi_j^T M \Phi_j} \quad (2)$$

In this expression, ω_j and Φ_j are the frequency and the mode shape for the *j*th mode, Δ denotes the change in the quantity that it precedes, ε_i stands for a transformation matrix to convert the local stiffness matrix of the *i*th element to global coordinates. M and k_i are the global mass matrix of the system and the stiffness of the *i*th element. To estimate the damage location, all previously compiled damage scenarios (database/characteristic) are compared with the damage case investigated (observed) [which may not in the database]

$$E = \frac{1}{N}\sum_{j,n}\left[\left(\frac{\Delta\omega_j^2}{\Delta\omega_n^2}\right)_{i\ Obs.} - \left(\frac{\Delta\omega_j^2}{\Delta\omega_n^2}\right)_{i\ Char}\right]^2 \quad (3)$$

In this expression, E stands for mean square error between observed (measured) and characteristic frequency change ratios, M stands for the number of members, sub-indices j and n stand for mode numbers, and the sub-index i stands for member number. The performance of the algorithm is tested through experiments performed on a welded steel frame and on a wire rope, and the results show that detecting damage location for one member is possible using natural frequency changes without using mode shapes. Moreover, for the transverse motion of wire rope natural frequencies and mode shapes are insensitive to damage and damping may be the only indication of distress. However, in these approaches, a slight error in the natural frequencies can cause big errors about the location of the damage.

In the Level 1 applications, mode shape and its derivatives are used, in which the second derivative of the mode shape is found to be sensitive to minor changes in the system: In [25] curvatures of mass-normalized mode shapes are used as a damage sensitive features and it is tested on finite element models of simply supported and cantilever beams to identify the damage existence and its location. Mode shape curvatures are calculated using the central difference approximation given by

$$\Phi''_{j,i} = \left(\Phi_{j,i+1} - 2\Phi_{j,i} + \Phi_{j,i-1}\right)/h^2 \quad (4)$$

where Φ stands for a mode shape, sub-indices j and i stand respectively for mode number and Degree of freedom (DOF) counters, $\Phi''_{j,i}$ denotes the central difference estimate of the curvature of the *j*th mode shape at the *i*th node, and h stands for the spatial distance between two consecutive nodes. A damaged member is detected using the maximum absolute difference between damaged and undamaged member mode shape curvatures calculated via

$$\Delta\Phi'' = |(\Phi^d)'' - \Phi''| \quad (5)$$

where the superscript d indicates that the mode shape belongs to the damaged system. The results show that mode shape curvature may localize the damage while mode shapes cannot localize it because mode shape identification needs several measurements from the structure, natural frequencies can be used to detect damage presence and the mode shape curvature method can be used to detect its location(s).

One of the original and promising recommendations in this regard is developed by Yuen [26] since the damage indicator contains both the mode shape and the natural frequency. In the study, a finite element model of a cantilever beam is examined. The damage in the cantilever beam was represented by the reduction of the modulus of elasticity. The following indicators were proposed to reflect well both the location and the size of the crack in the cantilever:

$$\Phi^*_{j,i} = \frac{\Phi^d_{j,i}}{\left(\omega^d_j\right)^2} - \frac{\Phi_{j,i}}{\left(\omega_j\right)^2} \tag{6a}$$

$$\theta^*_{j,i} = \frac{\theta^d_{j,i}}{\left(\omega^d_j\right)^2} - \frac{\theta_{j,i}}{\left(\omega_j\right)^2} \tag{6b}$$

In these expressions, Φ and θ are the mass normalized translational and rotational mode shapes, respectively; ω is the natural frequency; subindex j is the mode number; sub index i signifies the counter for the DOFs, superscript d shows that a parameter belongs to the damaged system. Although the mode number is indicated here by j, Eq. (6) is proposed by Yuen [26] only for the first modes. It should be noted that as in the study done by Pandey et al. [25], the parameters proposed by Yuen [26] are also dependent on baseline data.

Dong [27] applied the method [26] to a beam with both its ends fixed by using data from a finite element model established in line with the fracture theory, as well as using an experimental data set. It is shown that damage may be detected but not as conveniently as in the cantilever beam example in Yuen [26] and the efficiency of the method is increased by using the strain mode shapes.

2.2 Method Proposal

Detailed analysis is carried out on the promising method developed by Yuen [26]. As a result of many numerical analyzes, a new method has been developed in which the method has been simplified, the damage indicator has been modified and the damage can be identified by using both the individual mode and the sum of the modes. Moreover, the proposed method can be used for a different types of structures. In the proposed approach, mode shape is not normalized by mass matrix but it is normalized according to the reference DOF in Equation (5). With this simplification, it is not necessary to know or calculate the mass matrix. Moreover, instead of the eigenvalue (natural-frequency square) in the denominator, the value of the natural-frequency has been established and the difference between the DOF of the mode shape is used instead of the mode shape. The steps described and the proposed damage indicator can be summarized with the following equations:

$$\phi_{j,i} = \frac{\Phi^a_{j,i}}{\Phi_{j,R}} \tag{7}$$

$$\Delta\phi_{j,i} = \phi_{j,i} - \phi_{j,i-1} \tag{8}$$

$$\phi^*_{j,i} = \frac{\Delta\phi^d_{j,i}}{\omega^d_j} - \frac{\Delta\phi_{j,i}}{\omega_j} \tag{9}$$

In these expressions, $\Phi^a_{j,i}$ is the component of the arbitrarily scaled jth mode shape at the ith node, $\Phi_{j,R}$ is the value of the jth mode shape at the reference node, so that ϕ_j is scaled to have a unit value on the reference node. Since the damage indicator defined by Eqs. (7-9) is claimed to improve Yuen's [26] proposal, a comparative study is provided in the next section. It should be noted that the damage indicator calculated by the rotational mode shape is named as the rotational damage indicator, the damage indicator calculated by the translational mode shape is called the translational damage indicator.

2.3. Comparison of the Initial Proposal with Yuen's Proposal

In this section, a Bernoulli-Euler cantilever beam with a uniform cross-section is used. The features and cross-sectional properties of the model, in which rotational and translational DOFs are defined for each element, are given in Figure 2.

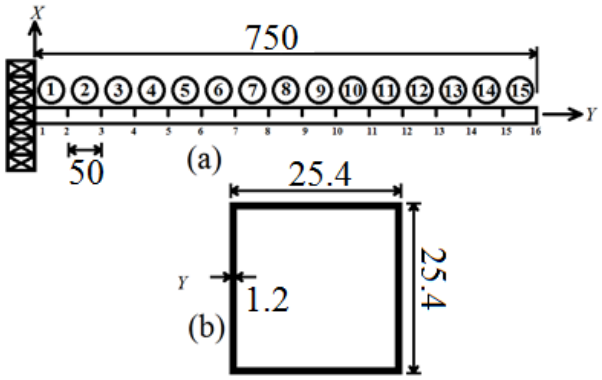

Figure 2. Cantilever beam model (a) finite element model with element and node numbers. (b) cross-section of the beam (all dimensions in mm).

Initially, modulus of elasticity is taken as $E = 208000\ \mathrm{N/mm^2}$ and the mass density is $\rho = 7.8\ \mathrm{kg/mm^3}$. Damage is defined as a decrease in the modulus of elasticity so that not the inertia but the stiffness matrix would change. The natural frequencies and mode shapes are calculated by solving the eigenvalue problem of the damaged and undamaged systems.

First, for all members, the elastic modulus is dropped to its half for each element one by one, and it is seen that both damage indicators in Yuen [26] correctly indicate the damage location. The translational eigen-parameter changes slope and the rotational damage indicator takes a step jump on the damaged element for each case. As an illustrative example, Figure 3 shows the damage indicators given in Eq. (6) for damage located on element 10.

As far as the proposed damage indicator defined by Eq. (9) is concerned, the damage indicator takes a positive value on the damages element while for other nodes it takes comparatively very small and sometimes even negative values as seen in Figure 4.

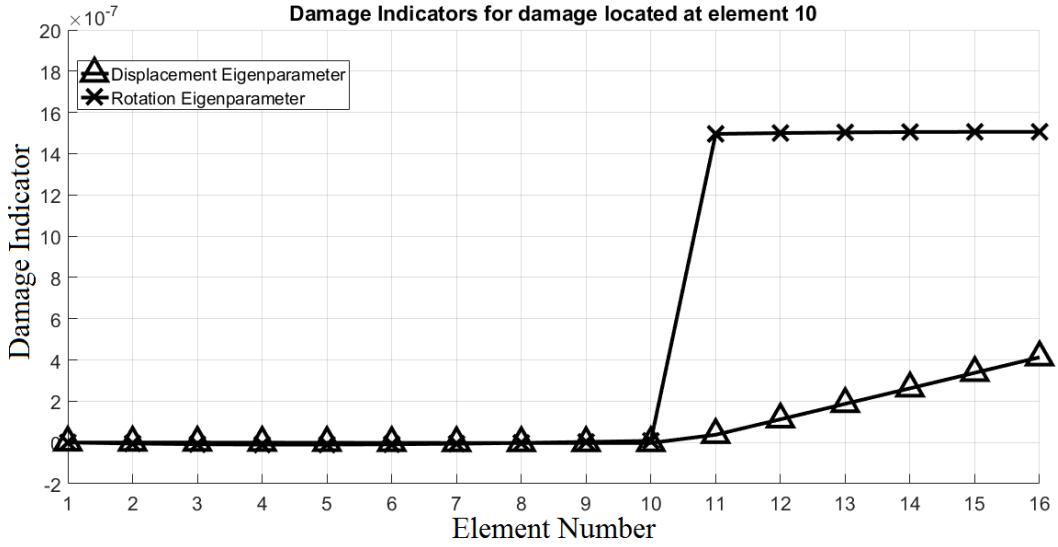

Figure 3. Yuen's [26] damage indicators for damage located on element 10.

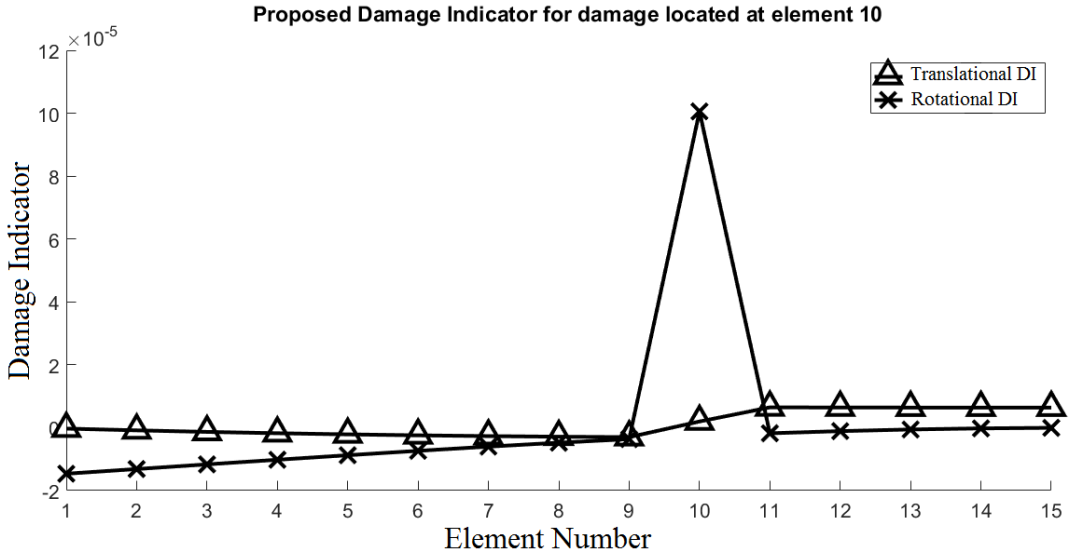

Figure 4. Proposed damage Indicators for damage located on element 10.

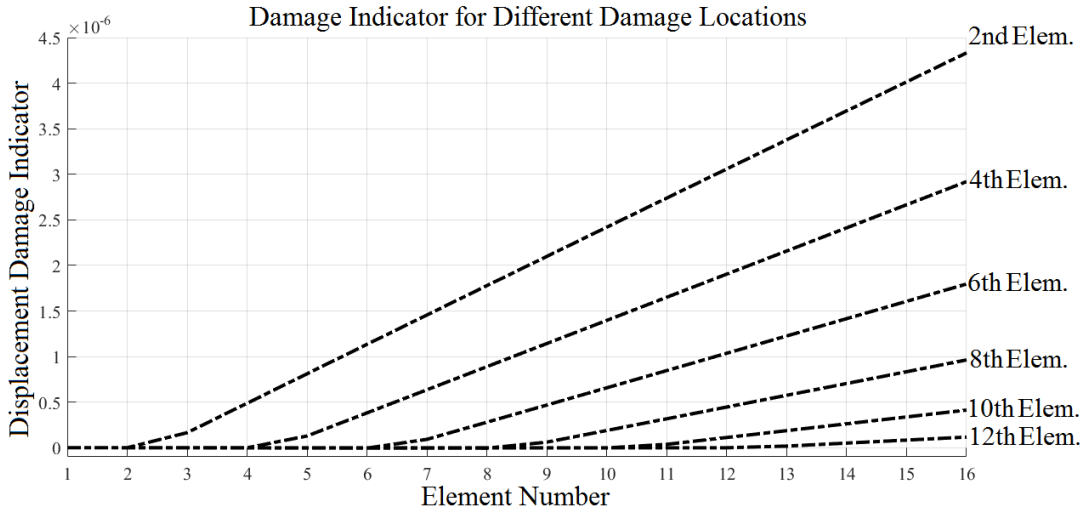

Figure 5. Proposed translational damage indicator for different damage locations.

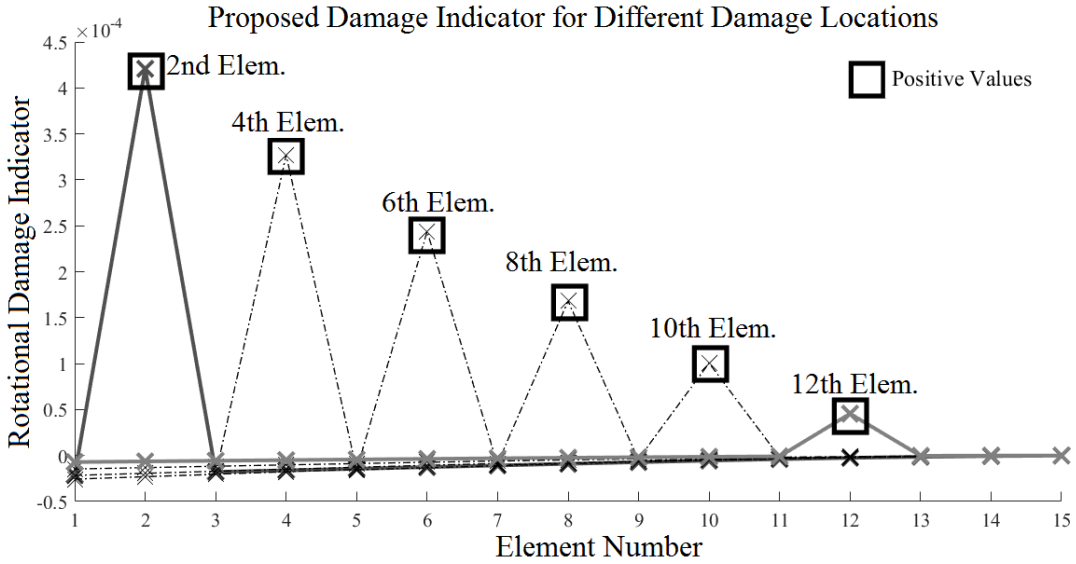

Figure 6. Proposed rotational damage indicator for different damage locations.

Figure 5 shows that the displacement eigen-parameter changes slope between nodes where damage locates and the slope becomes steeper afterward and remains constant to the tip of the cantilever.

The proposed rotational damage indicator takes a positive value between the nodes where damage is located while it is very small or negative on other elements as seen in Figure 6.

For this example, the damage indicators proposed by Yuen [26] can detect damage; however, the proposed damage indicator after the first improvements is still superior because there is no need to use mass normalized mode shapes in the proposed indicator,

Both the parameters used in Yuen [26] (Eq. (6)) and the proposed first improvements (Eq. (9)) may only be used in the detection of damage in a fix-free chain (sequential spring-mass) model with the first mode information since for the first mode of such a model, the differences between the mode shape components across the nodes keep the same sign (the first mode shape is monotonically increasing). To use the damage indicator for other modes and different boundary conditions, the second set of improvements as discussed below are required.

2.3 Further Enhancements

With the second enhancement procedure, the damage indicator is modified and damage can be identified by using either an individual mode or a cumulative set of modes. Moreover, it is shown that the proposed method can be used for the mass-spring systems with different end conditions.

The damage indicator calculated by Eq. (9) is not compatible with a mode shape containing 'saddle points' i.e. a region where the mode shape difference calculated via Eq. (8) alters the sign. To use the proposed approach in such cases, the mode shapes are first transformed into increasing functions and the same process is adapted. After this transformation, the damage indicator may be meaningfully calculated for any mode. Damage detection, however, is negatively affected if damage occurs on regions containing saddle points since there the difference calculated over the transformed mode shape change would be zero.

To calculate the proposed damage indicator using any mode, the following steps should be followed:

i. To convert the mode shape to an increasing function, the absolute value of the mode shape difference is used and these differences are summed:

$$\Delta\Phi_{j,i} = \left|\Phi_{j,i} - \Phi_{j,i-1}\right| \tag{10}$$

$$\tilde{\phi}_{j,i} = \sum_{k=1}^{i} \Delta\Phi_{j,k} \tag{11}$$

ii. To apply the proposed method for damage identification via the calculated mode-shape like $\tilde{\phi}_j$ vector, the vector is normalized by its value $\tilde{\phi}_{j,R}$ at the reference DOF and the differences of the normalized vector relative to the DOFs are calculated

$$\breve{\phi}_{j,i} = \frac{\tilde{\phi}_{j,i}}{\tilde{\phi}_{j,R}} \tag{12}$$

$$\Delta\breve{\phi}_{j,i} = \breve{\phi}_{j,i} - \breve{\phi}_{j,i-1} \tag{13}$$

iii. With these changes made in the damage parameter calculated using Equation (9-12), it has become possible to use other modes in damage identification.

$$\phi^*_{j,i} = \frac{\Delta\breve{\phi}^d_{j,i}}{\omega^d_j} - \frac{\Delta\breve{\phi}_{j,i}}{\omega_j} \tag{14}$$

All modes can be evaluated separately, or the damage parameter can be used as a total of the first-two or the first-three modes on a mode basis. On the other hand, as the number of modes increases, the number of the saddle points also increases and such saddle points adversely affect damage detection, so the use of the first two or three modes is recommended. To take into account different modes simultaneously, the cumulative damage indicator ϕ^*_i is defined as

$$\phi^*_i = \sum_{j=1}^{n_m} \left(\frac{\Delta\breve{\phi}^d_{j,i}}{\omega^d_j} - \frac{\Delta\breve{\phi}_{j,i}}{\omega_j} \right) \tag{15}$$

where n_m denotes the number of modes that will be included in the calculations of the index. Both damage indicators may be normalized by their maximum values as

$$\bar{\phi}_{j,i} = \frac{\phi^*_{j,i}}{\max_i \phi^*_{j,i}} \quad \text{or} \quad \bar{\phi}_i = \frac{\phi^*_i}{\max_i \phi^*_i} \tag{16}$$

For ease of reference, Eq. (14), or its scaled equivalent given as the first expression in Eq. (16), will be referred to as the 'single-mode damage indicator' whereas Eq. (15), or its scaled equivalent given as the second expression in Eq. (16), will be referred to as the 'multi-mode damage indicator'. It should be noted that by the normalization step in Eq. (16), information regarding the extent of damage is lost. Another important issue is that if rotations are explicitly defined as DOFs, a rotational modal shape may be used instead of translational mode shapes.

Since the proposed damage indicators are associated with how the mode shape changes across nodes, it is possible to say that the probable damage is between the detected measurement point and the previous measurement location. For the case where all DOFs are instrumented, damage between the nodes can be associated with the element number in the model. In case studies, both translational and rotational damage indicators are examined and it is found that the rotational damage indicator was more suitable for optimization. In case studies, both translational and rotational damage indicators are examined.

3. CASE STUDIES

The aim of each case study is to demonstrate the success of the damage indicator in closed systems and investigate the accelerometer mass loadings effect on the parameter. In the first case study, the position of damage is detected in a discrete with both translational and rotational damage indicators, and criteria to detect the damage in the closed system are shown for both parameters. In the second case study, the numerical proof has been made that the position of the damage can be determined with the rotational damage indicator according to the various modes and the various accelerometer mass. In the third case study, the effect of the accelerometer mass on the damage indicator was investigated as a solution to the problem encountered in the beam tip. The fourth case study, which is an experimental study, aims to determine the damage position in the segmented beam using the translation damage indicator. Since the accelerometer weights used are too large to be neglected relative to the beam mass and the total mass on the system does not change in the measurements, this system is considered a closed system. The accelerometer weight is compatible with the third case study and therefore this experimental study is complementary. In short, there are 2 important reasons for choosing the case studies in this study: 1) to examine the accelerometer weight effect and 2) to determine the damage location.

3.1. Case study I: Damage Identification in 15 DOF system

To investigate the possibility of the application of the damage indicator to such a problem, the proposed damage indicator will be tested for such a closed system in a numerical example where rotational and translational DOFs are defined for every element in the system. In other case studies in the article, systems for which rotational DOFs are inconsequential have been considered. Rotations may, however, be important for such a beam as used in the experimental work discussed at the end of this section, and therefore the rotational DOFs are included here.

The numerical model employed in this section is a 30 DOF system with 15 beam elements in series as shown in Figure 7. For every element, rotational and translational DOFs are defined at nodes. Section properties and modulus of elasticity of the beam elements are identical with the system used in the comparative study in section 2. The stiffness and mass matrices of each beam element are identical and in compliance with the Bernoulli-Euler beam model.

The mass of each accelerometer is equal to 1.25 times the translational mass of each piece. Four states of the system are considered (a) undamaged system, the system with (b) 50% reduction, (c) 75% reduction, and (d) 85% reduction in the modulus of elasticity of the 5th beam element.

Both unscaled and scaled equations are used when comparing the undamaged state and one of the damaged states of the system to locate the damage. For the unscaled first mode damage indicator defined in Eq. (14), the extent of damage can be detected as an increase in the damage indicator values as can be seen in Figure 8.

Figure 7 shows that when damage is at a single location, the damage indicator calculated with the first rotational mode is positive for a damage location and is negative for undamaged locations. On the other hand, the translational damage indicator value changes the sign on the damage location. The damage indicator for the damaged element and for the higher numbered elements takes a positive value and negative in all previous locations.

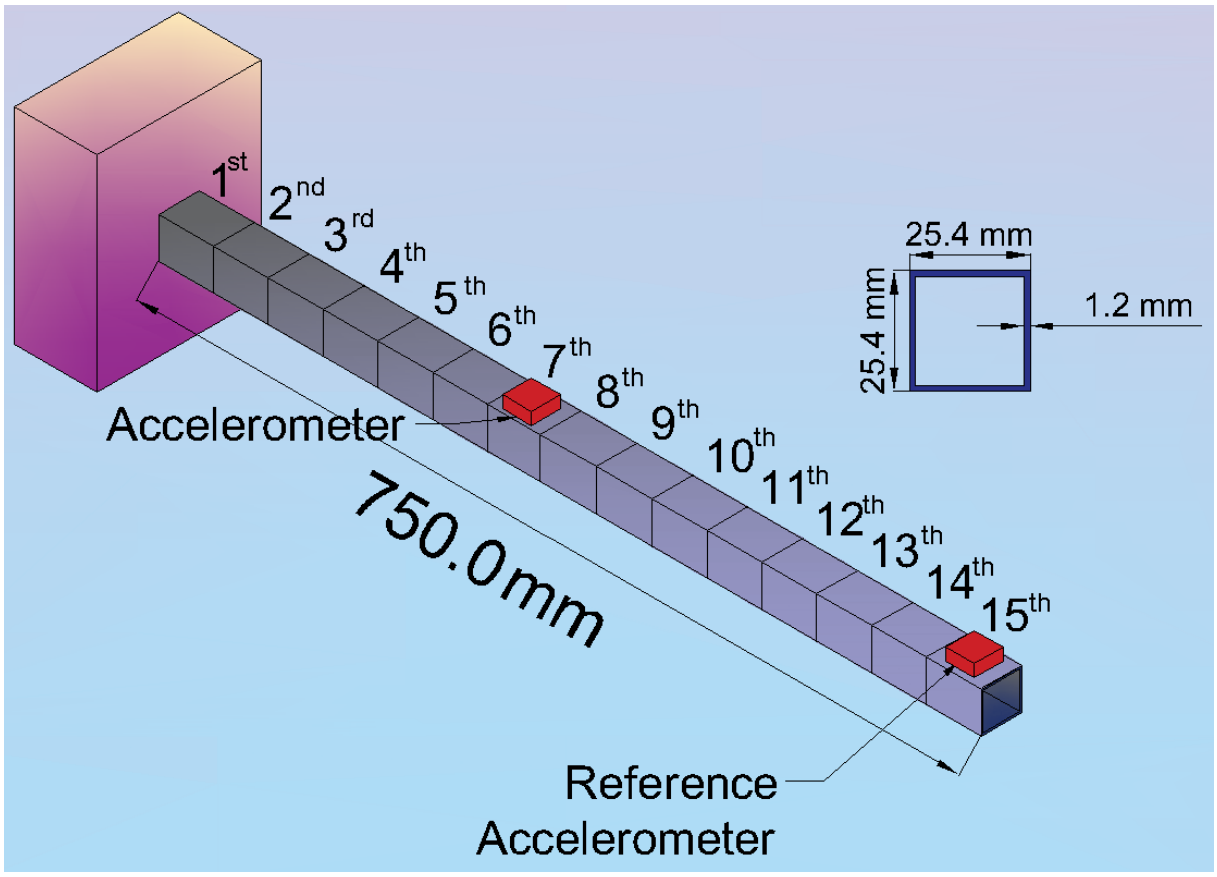

Figure 7. The beam model and the section properties

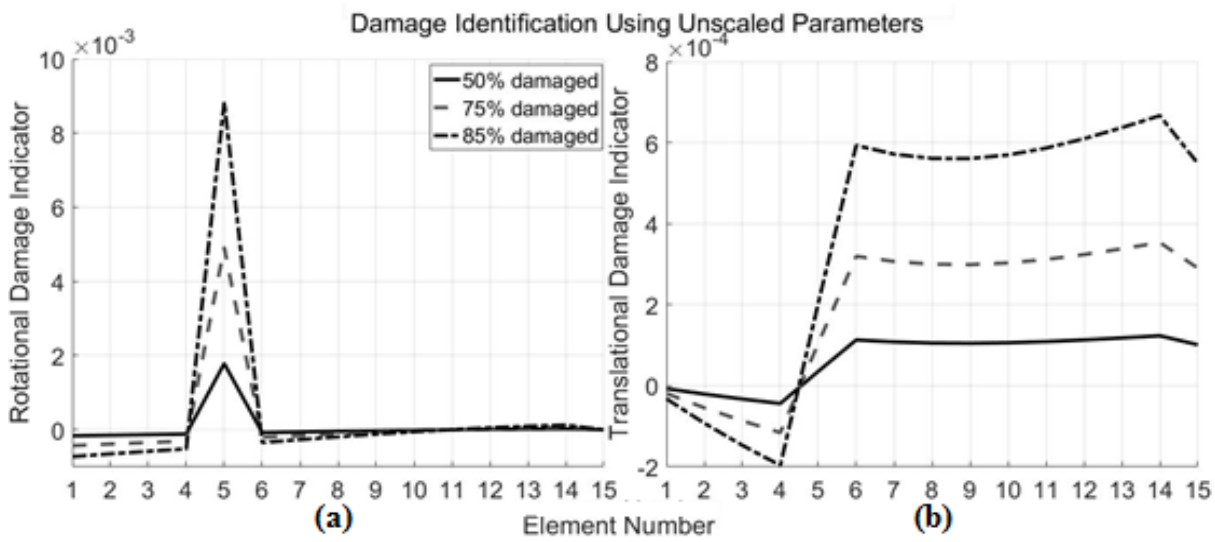

Figure 8. a) Rotational b) Translational Damage Indicator using Eq. (14).

3.2 Case study II: Numerical Proof of Damage Indicator in Closed Systems

A case of the known damage states and the known system where each variable can be accurately calculated is considered. The main aim is to examine the effectiveness of the proposed damage detection method under many damage conditions of a finite element of a cantilever beam model. The numerical model is a 200 DOF system with 100 beam elements in series as shown in Figure 9. For every element, rotational and translational DOFs are defined at nodes. Section properties and modulus of elasticity of the beam elements are identical with the system used in the previous case study. In console systems, the numbering is done from the fixed end to the free end. In the numerical proof, it is desired that all modal parameters are accurate and that possible errors due to the system identification step do not play a role. Therefore, natural-frequency and mode shapes have been found by solving the eigenvalue problem of the related systems. Firstly, the modulus of elasticity of each element is reduced one by one and the damage position was determined in the case of 5% stiffness reduction

(damage). The fact that the magnitude of the value obtained in the damage position is several times greater than the value obtained in the undamaged positions, enables the damage location to be easily identified.

The damage indicator value of the damaged element calculated using Eq. (16) is always 1. In cases where each element is damaged separately, the largest and the smallest values of the damage indicator taken other than the damaged position are plotted in Figure 10. In this way, the horizontal axis indicates the position of the damage; the vertical axis shows the largest and smallest values of the damage indicator in undamaged positions. It is understood that the value of the damage indicator in the damaged position in each case is approximately 60-100 times greater than values in the undamaged locations omitting the element at the free end and 6 to 20 times greater than values in the undamaged locations at the element at the free end. It is observed that the damage indicator interval for the undamaged elements varies according to accelerometer mass. As the accelerometer mass increases near the free end, it is observed that this range expands and the positive values get closer to the highest value. However, it is seen that the element at the free end receives the greatest damage indicator value at the value with the lowest accelerometer mass.

The first mode damage indicator, the first two modes, and the first three modes damage indicators are calculated for all damage cases using Eqs. (14-16). In the elements between 11/20 and 16/20 part of the beam, the damage indicator interval is higher in the first mode damage indicator, while it is close and lower in the other two damage indicators as can be seen in Figure 11. However, the first mode damage marker appears to be more reliable between the 16/20 of the beam and the free end. Between the fixed end and the 11/20 of the beam, all three damage indicators are calculated very close to the values.

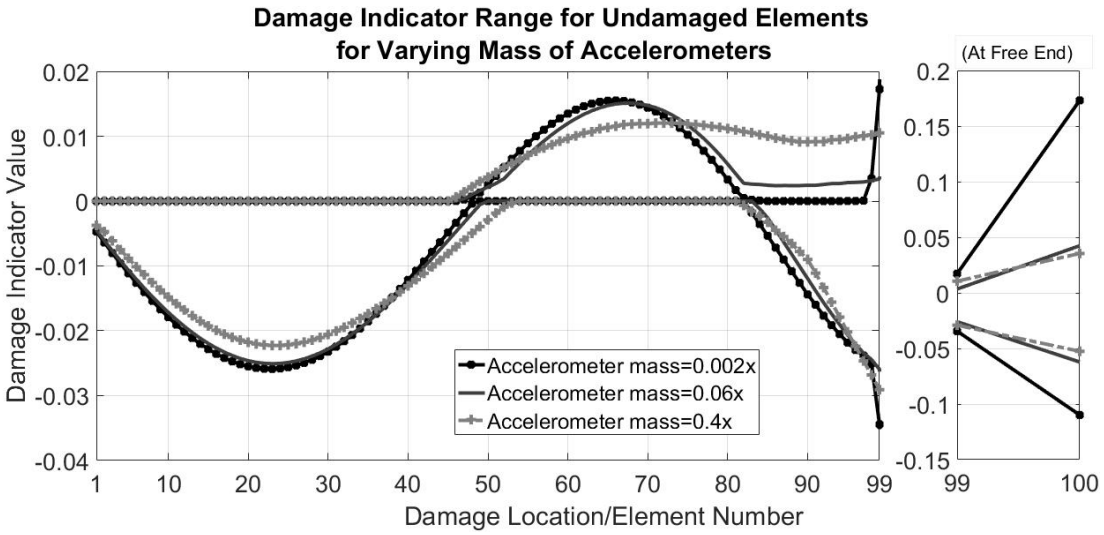

Figure 10. Damage Indicator Range for Undamaged Elements for Varying Mass of Accelerometers

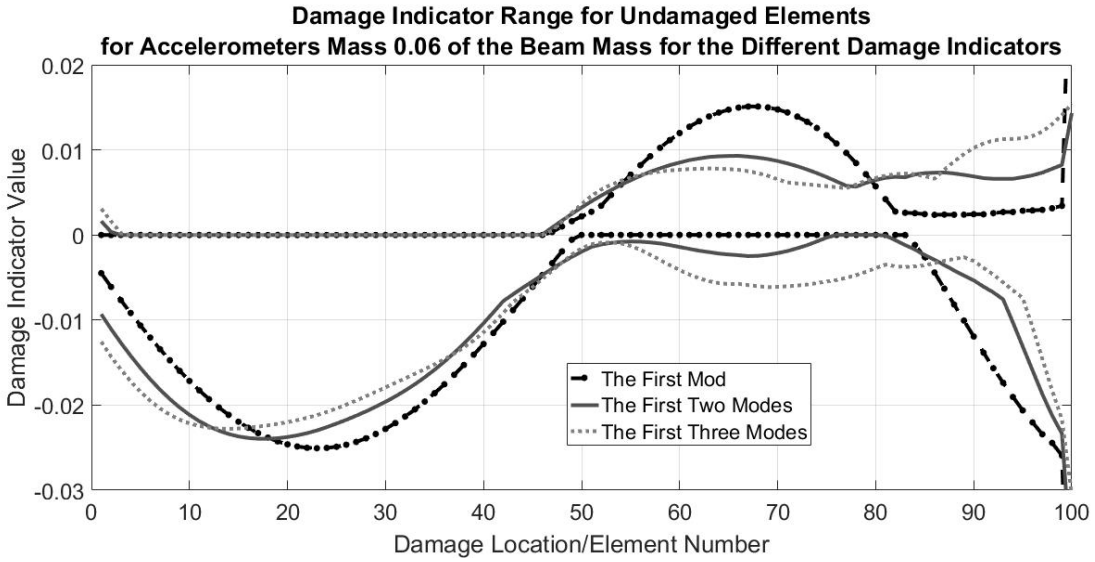

Figure 11. Damage Indicator Range for Undamaged Elements for Varying Accelerometers Mass 0.06 of the Beam Mass for the Different Damage Indicators.

3.3. **Case study III: Accelerometer Mass Effect**

In this section, damage detection based on different damage parameters and accelerometer mass is investigated for the element at free end. In the previous section, in case the element at the free end is damaged, in contrast to what is expected, the largest undamaged element damage parameter value (error) for the lowest mass accelerometer was seen. For this reason, at the free end, the error is compared according to the mass of the accelerometer according to the damage indicator values in Figure 12. In determining the damage in the last element by utilizing the first mode damage indicator, the error increases as the accelerometer weight decreases. However, in cases where the accelerometer mass is 0.08 times heavier or more than the mass of the beam, the first mode and the first two modes seem to behave similarly and they are better damage indicator than the third damage indicator. While the accelerometer weight is 0.08 times smaller than the weight of the beam, the first two and first three modes damage indicators appear to have fewer errors than the first mode damage indicator.

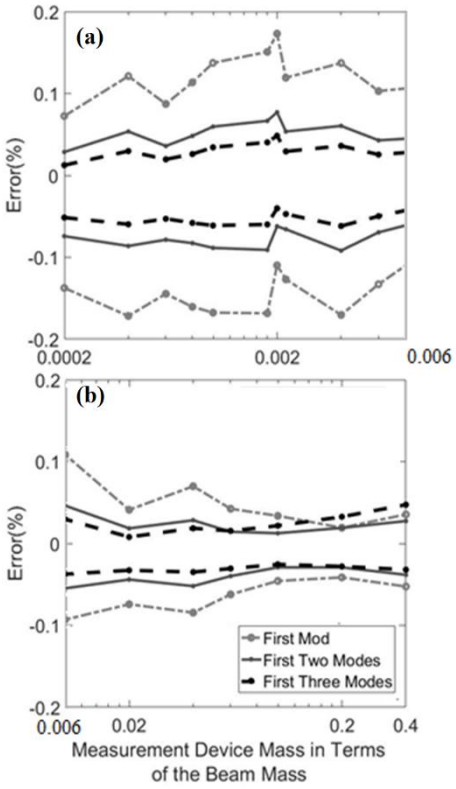

Figure 12. Accelerometer Mass (a)0.0002-0.006 (b) 0.006-0.4 of Beam Mass (Accelerometer Loading Effect).

3.4 Case study IV: Experimental Cantilever Beam

The purpose of this experimental study is to determine the damage location in a closed system. In this study, 2 accelerometers, whose weight cannot be neglected according to the weight of the beam, were used and measurements were made in different configurations. The mass distribution of the system has changed due to the change in accelerometer position and the system is considered as a closed system.

The beam used in this study was divided into 9 approximately equal parts with a cut angle of 45^0 and reassembled with the help of nails and bolts (Figure 13) to examine different damage locations. The outer dimension of one side of the square cross section beam is 40 mm and the wall thickness is 1.8 mm on average. When bolts are loosened, slight sliding is possible along the connection zone. This small sliding in turn leads to a reduction in the interaction area as shown in Figure 13. As the interaction or friction surface is reduced, local damping also decreases.

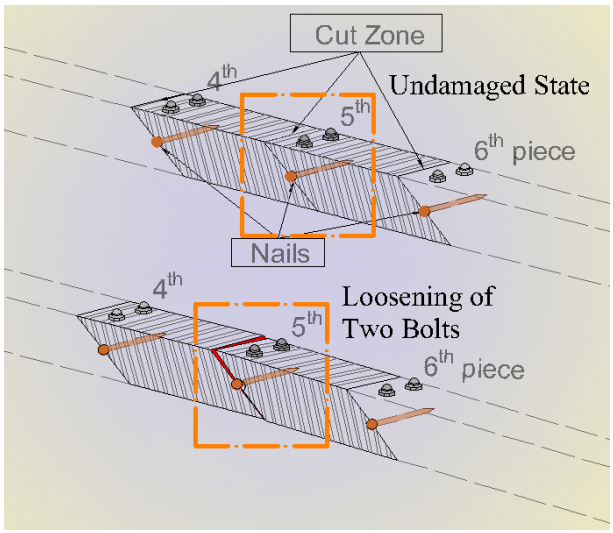

Figure 13. Damage Representation.

Due to their availability, the accelerometers used in this study are Kinematrix EpiSensor ES-U2 force balance uniaxial accelerometers. The weight of the accelerometer was measured as 346 grams and the weight of a single piece of the beam was 280 grams. For this reason, as mentioned above, the system is considered a closed system.

Damage to the system is defined as loosening two bolts on the 5th part from the fixed end. The location of damage is marked on the photograph of the specimen shown in Figure 14. The bolts are loosened to the level at which they can be further loosened by hand.

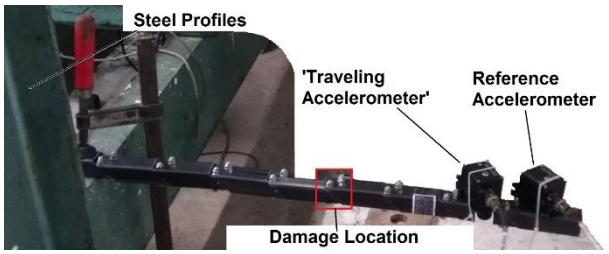

Figure 14. Experimental setup and the red box marks the damage position.

The specimen is instrumented with two uniaxial accelerometers aligned with the vertical, one of which is located on the last segment at the free end, and the second one being moved to a different segment at each test. For each setup, the duration of measurements is five minutes with a sampling rate of 200 Hz.

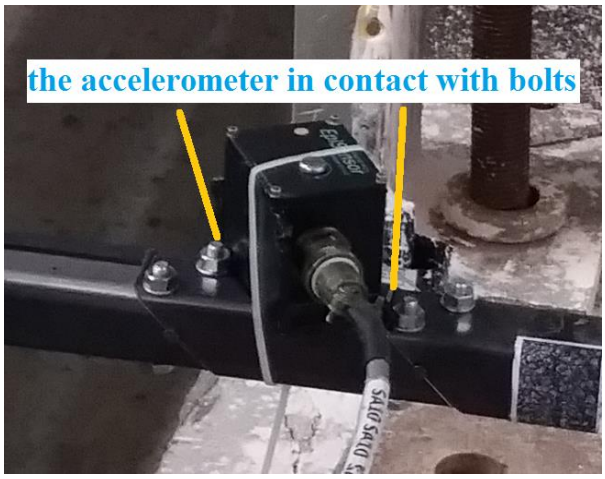

Figure 15. Accelerometer orientation.

The sensor located at the same location in all the tests is treated as and referred to as the 'reference accelerometer' while the second sensor is referred to as the 'traveling accelerometer'. The accelerometers are attached to the beam with hinges as shown in Figure 15.

The measurements are done in the following order:

Before damage: segment 7, 6, 5, 4, 3, 2, and 1

After damage: segment 1, 2, 3, 4, 5, 6, and 7

The system is excited by ambient inputs. In the last 9 measurements, steel profiles were tapped lightly and periodically with a finger. The purpose of this is to examine whether the damage indicator changes according to the change of external force intensity.

Only translational responses are measured and the rotations are not measured in the experimental study. The translational damage indicator value is expected to be positive starting from the damaged element to the tip element and will be negative between the damaged element (omitted) and the support.

It is important to note that the natural frequencies and mode shapes have been found by solving the eigenvalue problems of the systems. Since the mass matrix is dependent on the location of the second sensor, the natural frequencies of the system also depend on this location (see Table 1). Because the traveling accelerometer and the reference accelerometer are not located on the same segment (on the last segment at the free end of the beam), the same natural frequency values are used for the element at the tip and the element closest to the tip element.

For the time-domain method, first-order dynamic models were established with O3KID and ERA methods and the model order is set to 400. The data was divided into 25-second data with an 89% overlap and for each piece of data, a total of 390 frequencies between 0-100 Hz and corresponding mod-shapes values are calculated and the modal plot is constructed. For the frequency domain method, the data was divided into 20-second data with an 88% overlap. Fast Fourier transform (FFT) of the response is used, a total of 4096 modal parameters are estimated between 0-100 Hz. According to the ± 0.04 tolerance limit for the modal variables, the counts for each estimate are calculated. The mean values of peaks and estimates within the tolerance limit are given in Table 1. The translational mode shape of the damaged and undamaged systems are given in Table 1 and in Figure 16. The translational damage indicator is also given in Figure 17. The sign change is observed at the fifth element which is the damaged element as in the expectations. It is observed that the damage is in the 5th element with both time and frequency domain methods used. Based on the observations regarding this example, it is evident that rotational mode shapes should be measured if rotational DOFs contribute significantly to the dynamic response. It is possible, however, to detect damage using the translational damage indicator alone. The results also indicate that unscaled damage indicators should be preferred as they may lead to comparative estimates of the extent of damage when consecutively applied on a system with varying damage extent.

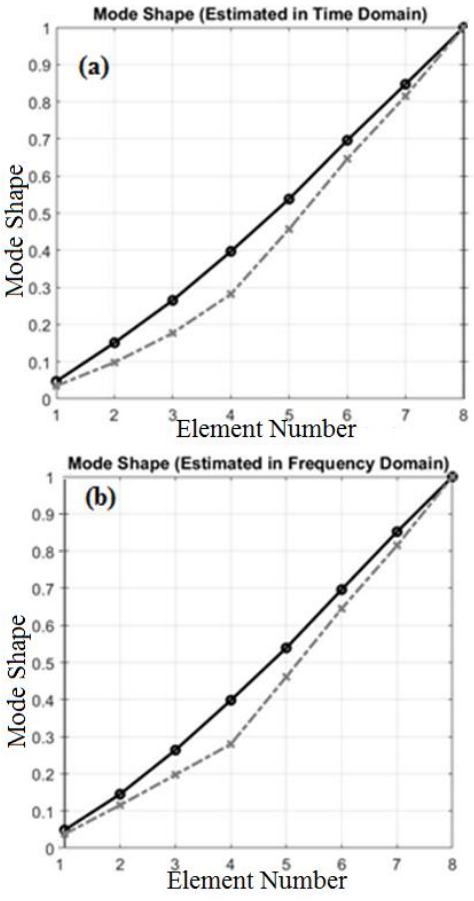

Figure 16. Mode Shape for two states of the system a)in time domain b) directly in frequency domain

Table 1. Estimated Modal Parameters for the First Mode

	Undamaged				**Damaged**			
	Time Domain		**Frequency Domain**		**Time Domain**		**Frequency Domain**	
Element Number	**Natural Freq.**	**Mode Shape**	**Natural Freq.**	**Mode Shape**	**Natural Freq.**	**Mode Shape**	**Natural Freq.**	**Mode Shape**
1	11.083	0.047	11.012	0.049	9.204	0.035	9.041	0.038
2	11.093	0.151	11.139	0.145	9.22	0.098	9.116	0.116
3	10.91	0.265	10.917	0.264	9.195	0.177	9.037	0.198
4	10.754	0.397	10.746	0.398	8.918	0.282	8.936	0.28
5	10.523	0.538	10.503	0.539	8.987	0.457	8.962	0.461
6	10.341	0.696	10.33	0.696	8.714	0.646	8.719	0.645
7	10.095	0.847	10.087	0.852	8.714	0.815	8.72	0.815
8	10.095	1	10.087	1	8.714	1	8.72	1

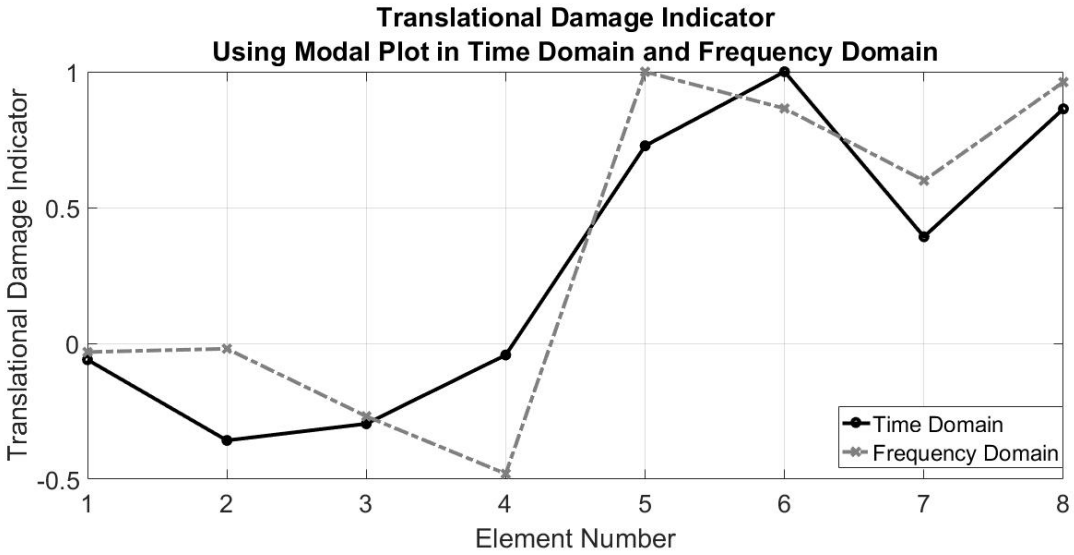

Figure 17. Location of damage using Translational Damage Indicator for the experimental study.

5. CONCLUSIONS

This study has three important objectives: (i) to show that an existing damage parameter in the literature also applies to closed systems, (ii) to examine the effect of the accelerometer mass used on the damage parameter, and (iii) to construct the modal plot with frequency domain methods.

Firstly, in the system identification section, the modal plot and count plot method are explained and it is stated that the modal plan method can also be constructed with frequency domain methods. In the experimental study in the fourth section, the modal plots and count plots are constructed separately with Fast Fourier Transforms in frequency-domain and, O3KID followed by ERA method in the time domain, and modal parameters were estimated in each domain.

In the damage detection section, a valid method for constant mass distribution systems is discussed for systems. The aforementioned method is compared with Yuen s method, which is its basis. Two numerical case studies have been carried out to show that this method is also valid for closed systems. Firstly, the damage indicator is tested according to the translation and rotation modes for a 15 element 30 DOF system. It has been shown that damage can be detected for both translational and rotational modes and related criteria are specified. Accordingly, for the translational modes, the position of the damage is defined as the element in which the damage parameter changes from negative to positive. For rotational modes, the element with the highest positive damage indicator value is shown to be damaged. Then, for the 100-element and 200-freedom built-in system with translational and rotational modes, it has been shown that it is possible to detect the damage in any position by using only rotation modes.

In addition, the effect of the mass of the accelerometer on the damage determination is investigated in numerical studies. Three different damage parameters are used: the first mode, the first-two modes, and the first three modes

damage indicators. For all sections of the beam, the least error is observed by utilizing the first-two mode damage indicator. It is observed that the accelerometer mass does not have a serious effect if the damage is between the middle element and the fixed part. In the other half, if the ratio of the accelerometer mass to the beam mass is 0.4, it is observed that the damage determination is adversely affected. It is suggested that if the damage is in the free end element, the accelerometer mass can be more than 0.08 times the mass of the beam.

NOMENCLATURE

E	the modulus of elasticity
ρ	mass density
Φ	mass normalized translational mode shapes
θ	mass normalized rotational mode shapes
ω	the natural frequency
$\tilde{\phi}_{j,R}$	the normalized damage indicator
ϕ_i^*	the cumulative damage indicator

ABBREVIATIONS LIST

SHM	Structural Health Monitoring Systems
FRF	Frequency Response Function
ID	Identification
O3KID	Output-only Observer filter ID.
DOF	Degree of freedom
ERA	Eigensystem Realization Algorithm

ACKNOWLEDGEMENTS

This research was funded by a grant from the İstanbul Medeniyet University Organization of Scientific Research Grant No. F-BEK-2020-1685.

DECLARATION OF ETHICAL STANDARDS

The author(s) of this article declare that the materials and methods used in this study do not require ethical committee permission and/or legal-special permission.

AUTHORS' CONTRIBUTIONS

Tarık TUFAN: Performed the experiments and analyse the results.

Hasan KÖTEN: Made general improvements. His suggestions, especially to the damage assessment part of the article, led to further development.

CONFLICT OF INTEREST

There is no conflict of interest in this study.

REFERENCES

[1] Aktan, A.E., Farhey, D.N., Brown, D.L., Dalal, V., Helmicki, A.J., Hunt, V.J. and Shelley, S.J., "Condition assessment for bridge management", **J. Infrastruct. Syst.**, 2(3), 108-17, (1996) https://doi.org/10.1061/(ASCE)1076-0342(1996)2:3(108).

[2] Tufan, T., "An investigation of system identification and damage estimation using modal plots, count plots and a damage indicator", **Ph.D. Dissertation, Bogazici** University, Istanbul, (2020).

[3] Reynders, E., "System identification methods for (operational) modal analysis: review and comparison", **Archives of Computational Methods in Engineering**, 19(1), 51-124, (2012).

[4] Tufan, T., Akalp, S., "Modal plot—System identification and fault detection", **Structuctural Control and Health Monitoring**, e2347, (2019).

[5] Vicario, F., Phan, M. Q., Betti, R., Longman, R. W., "Output-only observer/Kalman filter identification (O3KID)", **Structural Control and Health Monitoring**, 22(5), 847-872, (2015).

[6] Doebling, S.W., Farrar, C.R., Prime, M.B. and Shevitz, D.W., "Damage identification and health monitoring of structural and mechanical systems from changes in their vibration characteristics: a literature review", Research Report No. LA-13070-MS; **Los Alamos National Lab**, NM, United States, (1996).

[7] Medhi, M., Dandautiya, A., & Raheja, J. L., "Real-time video surveillance based structural health monitoring of civil structures using artificial neural network", **Journal of Nondestructive Evaluation**, 38(3), 63, (2019).

[8] Eroğlu, Y., Seçkiner S. U., "Early fault prediction of a wind turbine using a novel ANN training algorithm based on ant colony optimization", **Journal of Energy Systems**. 3(4), 139-147, (2019).

[9] Azimi, M., Eslamlou, A. D., & Pekcan, G. "Data-Driven Structural Health Monitoring and Damage Detection through Deep Learning: State-of-the-Art Review", **Sensors**, 20(10), 2778, (2020).

[10] Yang, J.N., "Application of optimal control theory to civil engineering structures", **J. Eng. Mech. Div.ASCE**, 101(6), 819-838, (1975).

[11] Ren, W.X. and Zong, Z.H., "Output-only modal parameter identification of civil engineering structures", **Structural Engineering and Mechanics**, 17(3-4), 429-444, (2004). http://dx.doi.org/10.12989/sem.2004.17.3_4.429.

[12] Peeters B., "System identification and damage detection in civil engeneering", **Ph.D. Dissertation**, Katholieke Universiteit Leuven, (2000).

[13] Tufan, T, Köten, H., "Accelerometer Mass Loading Study Based on a Damage Identification Method using Fundamental Laws in Closed Systems", **8th Eur. Conf. Ren. Energy Sys.** (2020).

[14] Donadon, M. V., Almeida, S. D., & De Faria, A. R., "Stiffening effects on the natural frequencies of laminated plates with piezoelectric actuators", **Composites Part B: Engineering**, 33(5), 335-342, (2002).

[15] Yadav, A., & Singh, N. K., "Investigation for accelerometer mass effects on natural frequency of magnesium alloy simply supported beam", **Materials**

Today: Proceedings, (2020).

[16] Lehmann, T., "Some thermodynamical considerations on inelastic deformations including damage processes", **Acta mechanica** 79, no. 1-2: 1-24, (1989).

[17] Brünig, M., "An Anisotropic Continuum damage Model: Theory and Numerical Analyses", Latin American Journal of Solids and Structures 1, no. 2: 185-218, (2004).

[18] Rytter, A. "Vibrational based inspection of civil engineering structures". **Ph.D. Dissertation**, Aalborg University, (1993).

[19] Fassois, S. D. and Sakellariou, J. S., "Statistical Time Series Methods for SHM". In **Encyclopedia of Structural Health Monitoring**. (eds Boller, C., Chang, F. and Fujino, Y.), (2009). https://doi.org/10.1002/9780470061626.shm044.

[20] Ayres, J.W., Lalande, F., Chaudhry, Z. and Rogers, C.A., "Qualitative impedance-based health monitoring of civil infrastructures", **Smart Mater. Struct.** 7(5), 599, (1998). https://doi.org/10.1088/0964-1726/7/5/004.

[21] Gkoktsi, K., & Giaralis, A. "A compressive MUSIC spectral approach for identification of closely-spaced structural natural frequencies and post-earthquake damage detection", **Probabilistic Engineering Mechanics**, 60, 103030, (2020). https://doi.org/10.1016/j.probengmech.2020.103030

[22] Tran-Ngoc, H., Khatir, S., De Roeck, G., Bui-Tien, T., & Wahab, M. A. "An efficient artificial neural network for damage detection in bridges and beam-like structures by improving training parameters using cuckoo search algorithm", **Engineering Structures**, 199, 109637, (2019). https://doi.org/10.1016/j.engstruct.2019.109637

[23] Cawley, P. and Adams R. D., "The location of defects in structures from measurements of natural frequencies", **The Journal of Strain Analysis for Engineering Design**, 14(2), 49-57, (1979).

[24] Hearn, G. and Testa B. R., "Modal Analysis for Damage Detection in Structures", **J. Structural Engrg**., 117-10, (1991).

[25] Pandey, A. K., Biswas M., Samman, M. M., "Damage detection from changes in curvature mode shapes", **Journal of sound and vibration**, 145(2), 321-332, (1991).

[26] Yuen, M.M.F., "A Numerical Study of the Eigenparameters of a Damaged Cantilever", **J Sound Vib**, 103, 301–310, (1985). https://doi.org/10.1016/0022-460X(85)90423-7.

[27] Dong, C., Zhang, P.Q., Feng, W.Q. and Huang, T.C. The sensitivity study of the modal parameters of a cracked beam. **Proceedings of the 12th International Modal Analysis**, Schenectady, New York, USA, January, (1994).